Evaluation of standard compensation of thermal distortion caused by rotating spindle on volumetric measurement of a floor type machining centre

M. Okénka, M. Morávek, O. Horejš, M. Mareš
Czech Technical University in Prague, Faculty of Mechanical Engineering, Department of Production Machines and Equipment, RCMT, Horská 3, 128 00 Prague, Czech Republic

Abstract

A direct implication of recent increasing demands on machining accuracy is an effort to minimize errors by any possible means. Since a significant and possibly major part of error is caused by thermal deformation, its compensation has high priority. Various methods of thermal error compensation have been developed including a complex dynamic method using transfer functions. Such a method, with relatively minor calibration requirements, has proved to be reliable in the prediction of thermally induced error at one point of a machine tool workspace. This paper focuses on extending the compensation method usability across the machine tool workspace. A possibility of extrapolating the predicted deviation of a tool centre point in the direction of *Z* axis in the calibrated location to the whole workspace is examined. No additional gauges and external inputs are used. The concept results are applied to a volumetric measurement of the deviation of the tool centre point in the *Z* axis of a floor type machining centre that was submitted to a test sequence of thermal loads applied by various spindle rotational speeds. The concept has proven to be capable of increasing the quality of the thermal error compensation in comparison with the one point calibrated model.

1 Introduction

Since the heat generated and accumulated in the machine tool (MT) and its surrounding induces significant displacement of the tool centre point (TCP), there is a number of methods developed to more or less successfully compensate for

thermally induced error [1]. Passive methods such as thermally unresponsive or symmetric construction give limited results while being cost demanding. Active methods such as managing heat sources and sinks, active TCP position sensing, multi linear regression models or FEM based models offer partial solutions. However, cost effectiveness, robustness and ease of implementation are issues.

High quality thermal error compensation offers a transfer function (TF) based model while using no additional gauges and being easy to calibrate and integrate to a control system of a MT. A TF model was described in [2] and proven to be capable of high quality and robust thermal error compensation in the calibration point of the workspace of various types of MTs [3].

The major contribution to overall thermally induced error is distortion caused by heat produced by a rotating spindle [2]. According to the measurement carried out in [4], the error caused by the rotating spindle is articulated primarily in the direction of the rotational axis (*Z*). The paper also presented the inequality of the thermally induced error across the workspace of a MT. Thus the one point TF models (standard TF models) harbour an improvement potential.

2 Experimental setup

The experiment described subsequently aims to extrapolate the error estimation given by the standard TF model to the whole MT workspace using a low order relation to a motion axis position. The only applied load is spindle rotation and the investigated error is in *Z* direction since those are the main error source and the most significant error component [4], [5]. Additionally, as error caused by spindle rotation does not vary significantly over the workspace of mid–sized MTs, the measurement for the extrapolation verification took place on a heavy floor type MT (see Figure 1 depicting kinematic configuration of the floor type MT and placement of the temperature sensors).

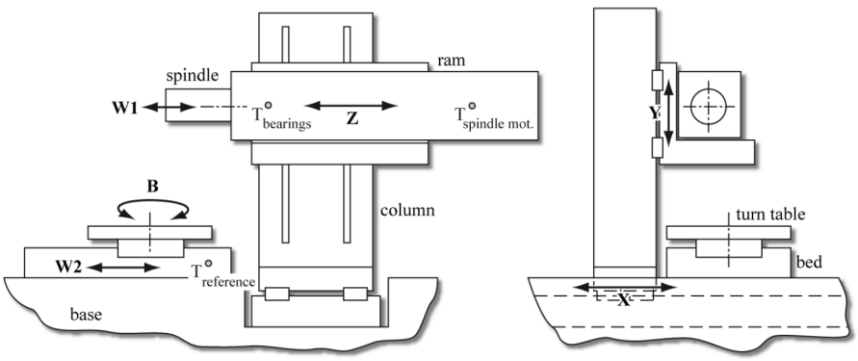

Figure 1: Kinematic configuration of a floor type MT with marked temperature sensor positions, [2]

Due to serial configuration of the MT, a linear distribution of TCP position error may be assumed and, furthermore, the dependency on *X* axis position should be limited as the *X* guideway is on a long and robust bed far from the heat source. Thus only *Y* and *Z* position are used for the extrapolation.

In Figure 2, the measuring device is depicted; calibrated spheres are placed across the workspace and periodically located using a self–centring head "MT-Check" (see [4], [5] for further details of the measurement method and the device).

Figure 2: Volumetric error measuring of 5-axis machining centre using MT-Check probe and calibrated spheres placed across the workspace [5]

When the MT is in thermo-dynamic equilibrium with its surrounding, spindle rotation is set to a constant speed and the displacement of the TCP is recorded at the coordinates of individual spheres during the heating process. The coordinates are given in Table 1, Figure 3 depicts their positions in the workspace graphically.

Simultaneously with the TCP position measurement, temperature sampling took place at both the MT spindle and surroundings (Figure 1: $T_{\text{spindle mot.}}$ and $T_{\text{reference}}$). Both the TCP error and temperatures were recorded on a MT loaded by free spindle rotation at speed of 500 rpm and 2000 rpm respectively.

Table 1: Position of individual reference spheres

	X	Y	Z
Sphere	[mm]		
1	2628	-794	-1126
2	2628	-1441	-1112
3	2633	-2111	-1108
4	3026	-1731	-620
5	3220	-789	-416
6	3225	-2111	-412

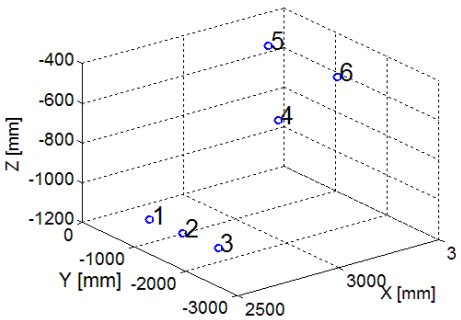

Figure 3: Plotted position of individual reference spheres

3 Calibration and modelling

Extrapolation of the predicted error from one point to the whole workspace is based on the assumption of linear thermal error dependency on the motion axis position. Therefore, the ratio b of given deformations at individual coordinates should be a constant and the following relation would describe the deformation across the workspace:

$$\Delta \boldsymbol{Z_j} = b_j \, \Delta \boldsymbol{Z}_{cal} \qquad \text{(eq. 1)}$$

where $\Delta \boldsymbol{Z}$ stands for the time vector of the Z deformation at point j, b_j for linear coefficient and $\Delta \boldsymbol{Z}_{cal}$ stands for the time vector of predicted deformation of the TCP at the point of calibration of the TF model.

Once the coefficients b_j are known at a number of different coordinates of the workspace, it is possible to obtain its value at an arbitrary point of the workspace by linear interpolation. To minimize calibration requirements, 4 of the measured points were chosen to obtain corresponding b_j coefficients (spheres number 1, 3, 5, 6 in Figure 3). Points number 4 and 6 serve as control points for interpolation. The TF model was calibrated at point 4 (based on test with spindle rotational speed of 500 rpm).

The TF model extrapolation is then verified under non-calibration conditions (tested with spindle rotational speed of 2000 rpm).

For practical thermal error compensation, a more complex TF model is needed, covering differences of heating and cooling processes and respecting alternations of the thermal MT behaviour due to various thermal loads. Nevertheless, the aim of this research is to investigate regularity of error dispersion due to thermal load of the rotating spindle. Thus only the heating process is taken into consideration. Concept of the TF model itself has been proved [3].

First, the one–point TF model was calibrated at point number 4 on the MT loaded by spindle rotation of 500 rpm. The only inputs used for the model are temperatures of the spindle motor and the MT surroundings ($T_{\text{spindle mot.}}$, $T_{\text{reference}}$). See Figure 4 comparing the measured value of Z deformation at the point 4 and the value predicted by TF model. The model follows the measured data perfectly and under similar conditions should provide solid source data for extrapolation to the MT workspace.

The norm fit (eq. 2) is used to quantify the quality of the estimation:

$$fit = \left(1 - \frac{\left\|\Delta \boldsymbol{Z} - \widehat{\Delta \boldsymbol{Z}}\right\|}{\left\|\Delta \boldsymbol{Z} - \overline{\Delta \boldsymbol{Z}}\right\|}\right) \cdot 100 \qquad \text{(eq. 2)}$$

where $\Delta \boldsymbol{Z}$ stands for measured value of Z deformation, $\overline{\Delta \boldsymbol{Z}}$ for its arithmetic mean over time and $\widehat{\Delta \boldsymbol{Z}}$ stands for the value estimated by the TF model or its extrapolation, $\|\boldsymbol{x}\|$ marks Euclidean norm.

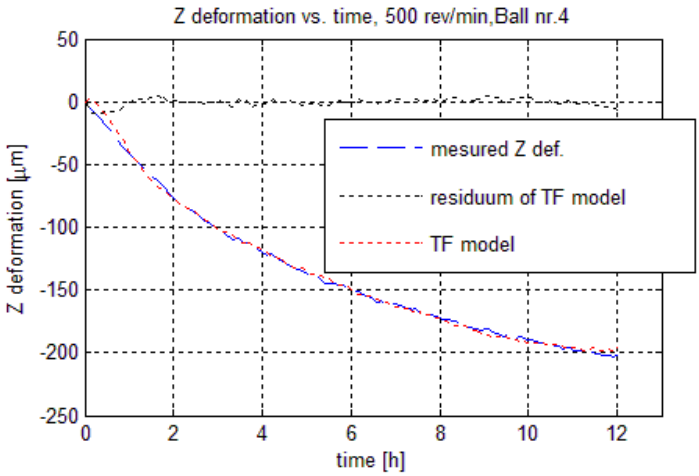

Figure 4: Measured Z component of deformation at point 4 compared to value predicted by the TF model calibrated at the same point, black dotted line marks difference (residual error), $fit = 94.4\%$

3.1 Extrapolation

For extrapolation of the deformation predicted by the standard TF model (see Figure 4), the b_j coefficients were obtained from measured data as arithmetic mean over time of ratio of *Z* deformation of individual spheres to *Z* deformation of the sphere number 4 (eq. 1, Figure 3). The b_j values are presented in Table 2 for test with constant spindle rotation of 500 rpm. Note that the ratios of *Z* deformation of individual spheres are close to 1. Nevertheless compensating for those residual differences might further improve performance of single point models in MT workspace by avoiding such divergence.

Table 2: Value of coefficients b_j for individual measuring spheres for 500 rpm

Ball nr. "j"	1	2	3	4	5	6
b_j	1.14	1.14	1.08	1	0.97	0.9

By multiplying the predicted value of the TF model (Figure 4) by the corresponding b_j (Table 2) accordingly to eq. 1, the extrapolated values can be plotted and compared to values measured at each point and to the value given by the standard TF model. For corner spheres, the extrapolated value uses directly the known coefficients (Figures 5; spheres a) 1, b) 3, c) 5, d) 6; coefficients b_1, b_3, b_5, b_6). Values for intermediate spheres (Figures 6; spheres a) 2 and b) 4) use coefficients obtained by linear interpolation from the corner four ones.

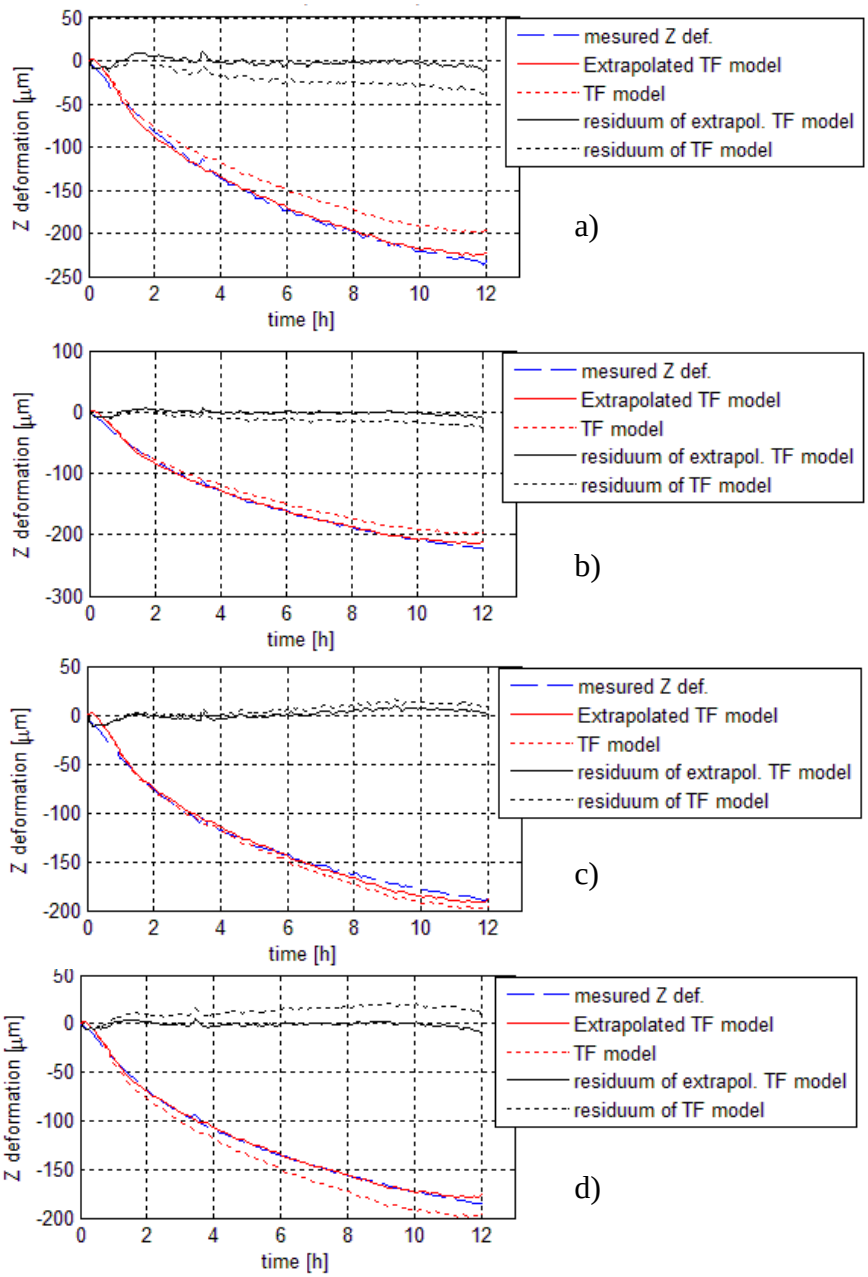

Figure 5: Measured Z deformation vs. time compared to extrapolated and standard TF model, accompanied by corresponding residua for individual spheres, 500 rpm

a) Sphere 1 b) Sphere 3
c) Sphere 5 d) Sphere 6

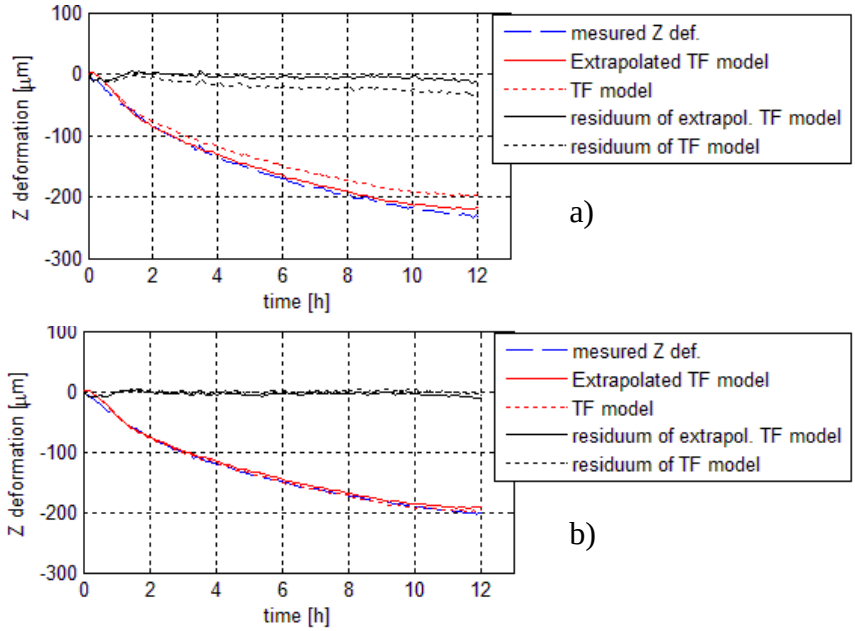

Figure 6: Z deformation vs. time, 500 rpm
a) Sphere 2 b) Sphere 4 – calibration point of TF model

Note that while the shape of the deformation progress is well estimated by the standard TF model, the absolute values are not met perfectly except for the calibration point. After compensation with the help of the model extrapolation (eq. 1) both the shape of error evolution and its absolute value are well estimated.

For residual error quantification, the peak-to-peak criterion (PK) is used as defined by following eq. 3.

$$PK = \left|\max\left(\Delta \boldsymbol{Z} - \widehat{\Delta \boldsymbol{Z}}\right) - \min\left(\Delta \boldsymbol{Z} - \widehat{\Delta \boldsymbol{Z}}\right)\right| \qquad \text{eq. 3}$$

Table 3: fit values and PK values for standard TF model and its extrapolation, applied load – 500 rpm, symbol PK stands for peak-to-peak value of the residual error, subscript *std TF* stands for standard TF model, *ext* for its extrapolation

500 rpm	fit_{ext}	$fit_{std\ TF}$	$max\|\Delta \boldsymbol{Z}\|$	PK_{ext}	$\frac{PK_{ext}}{max\|\Delta \boldsymbol{Z}\|}$	$PK_{std\ TF}$	$\frac{PK_{std\ TF}}{max\|\Delta \boldsymbol{Z}\|}$
sphere	[%]		[μm]	[μm]	[%]	[μm]	[%]
1	92.7	65.5	230	27.4	11.9	41.6	18.1
2	89.9	66.7	230	29.1	12.6	40.2	17.5
3	93.9	77.9	220	18.5	8.4	28.9	13.1
4	90.5	94.4	200	16.5	8.3	17.0	8.5
5	90.4	83.3	185	24.5	13.2	31.0	16.8
6	94.8	72.2	183	16.0	8.7	29.9	16.3
average	**92**	**77**	**208**	**22.0**	**10.5**	**31.4**	**15.0**

The extrapolated fit values are compared to the fit values obtained by the standard TF model in Table 3. Note that for all but the calibration point, the fit value is evidently increased. Approximate residual errors are presented on the right side of the Table 3.

4 Verification

The error estimation of the MT loaded by 2000 rpm was carried out to investigate the extrapolation and of the TF model under non-calibration conditions. Figure 7 a) depicts the best obtained result (on sphere 1) and Figure 7 b) the worst (on sphere 6). Table 4 shows fit values for standard TF model and its extrapolation.

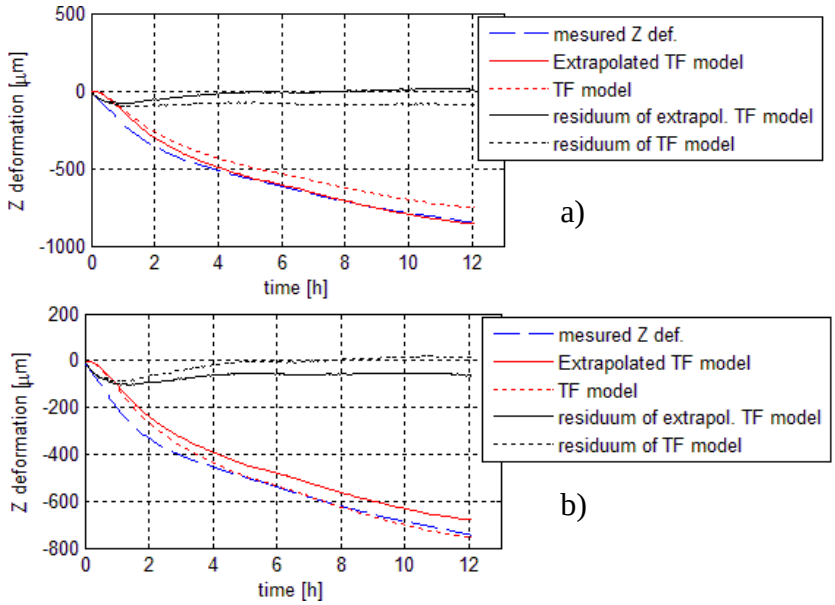

Figure 7: Z deformation vs. time, 2000 rpm
a) Sphere 5 – the best fit b) Sphere 6 – the worst fit

The TF model calibrated under 500 rpm is not capable of capturing the physical nature of heat progression for higher loads. Neither the absolute values of the TCP deformation nor the shape of the error development matches the measured values. Moreover, the used b_j (calibrated for 500 rpm) does not respect volumetric variance of the deformation. Thus estimated values do not match the measured values as closely as at 500 rpm. Still, a remarkable error compensation was obtained even in the worst case (average error reduction from 792 μm to 100.2 μm).

Table 4: fit values and PK values for the standard TF model and its extrapolation, applied load–2000 rpm

2000 rpm	fit_{ext}	$fit_{std\ TF}$	$max\|\Delta \boldsymbol{Z}\|$	PK_{ext}	$\frac{PK_{ext}}{max\|\Delta \boldsymbol{Z}\|}$	$PK_{std\ TF}$	$\frac{PK_{std\ TF}}{max\|\Delta \boldsymbol{Z}\|}$
sphere	[%]		[μm]	[μm]	[%]	[μm]	[%]
1	84.7	60.2	840	105.8	12.6	104.0	12.4
2	81.5	59.7	845	94.5	11.2	107.9	12.8
3	78.1	61.2	840	94.4	11.2	105.8	12.6
4	68.8	74.5	770	105.1	13.6	101.3	13.2
5	80.1	81.6	725	95.3	13.1	115.7	16.0
6	63.0	79.9	730	106.1	14.5	113.4	15.5
average	**76**	**70**	**792**	**100.2**	**12.7**	**108.0**	**13.7**

5 Conclusion

The extrapolation method described enables the standard one-point TF model for thermal error compensation to be used throughout the whole workspace. The thermal error time development due to a rotating spindle was found similar in shape across the workspace of the MT. Thus linear coefficients b_j facilitate residual error minimization.

Under calibrating conditions of the TF model and of the b_j, the fit value was increased by the extrapolation to over 90 % and the residual error was reduced to less than or equal to 29 μm (non-compensated error over 200 μm). The results under calibration conditions show that the assumption of (time consistently) linear error distribution can be utilised to expand the usability of standard compensation models.

The b_j values were not satisfactorily proven to be valid under conditions far from calibration since the TF model extrapolation did not enhance standard TF model performance across the whole workspace. While extrapolation decreased the approximation quality for spheres 4, 5, 6, it managed to limit the residual error under 106 μm (non-compensated error over 800 μm, standard TF model compensated error 104~115 μm). While the b_j is time consistent, it varies depending on the applied thermal load. Therefore multiple values should be found for individual basic load spectra. A new $b_{j\,2000}$ calibrated under high revolutions is presented in Table 5 accompanied with reached *fit* and *PK* (peak-to-peak of residual error) values.

Table 5: Value of coefficients $b_{j\,2000}$ for individual measuring spheres for 2000 rpm test accompanied with reached fit and PK values

Ball nr. "j"	1	2	3	4	5	6	average
$b_{j\,2000}$	1.06	1.07	1.06	1	0.93	0.96	
fit [%]	74.2	73.6	75.2	71.3	73.3	75.6	**73.9**
$PK_{ext\,2000}$	95.3	99.7	96.2	103.5	93.8	97.3	**97.6**

A comparison of Table 2 with Table 5 shows that the dependency on the motion axis position is reduced for higher revolutions. Additionally, comparison of Table 4 and Table 5 yields that the proprietary $b_{j\,2000}$ does not compensate for an insufficiently estimated evolution of the TCP displacement by the TF model (calibrated under 500 rpm). Nevertheless, a further reduction of the residual error from avg. $100.2\ \mu m$ to $97.6\ \mu m$ was obtained using the dedicated $b_{j\,2000}$. This indicates that every TF model for specified conditions (high/low revolution, heating/cooling) should be accompanied by proprietary b_j values. With such a combination, presumably the fit value attained may reach over 90 % for high revolutions as for low revolutions.

Future work in this vein should concentrate on including more thermal sinks and sources into the MT thermal behaviour description out of the calibrated point (axis movement, cutting process) and general extension of the portfolio of heavy-duty MTs with advanced thermal error compensation models.

Acknowledgement

This work was supported by the Grant Agency of the Czech Technical University in Prague, grant No. SGS16/220/OHK2/3T/12.

Reference

1. J. Mayr, J. Jedrzejewski, E. Uhlmann, M. Alkan Donmez, W. Knapp, F. Härtig, K. Wendt, T. Moriwaki, P. Shore, R. Schmitt, C. Brecher, T. Würz a K. Wegener, Thermal issues in machine tools, CIRP Ann.Manuf.Technol., Vol.. 61, n. 2, p. 771–791, 2012.

2. MAREŠ, M., HOREJŠ, O., HORNYCH, J. Advanced Thermal Error Compensation of a Floor Type Machining Centre Allowing for the Influence of Interchangeable Spindle Heads. Journal of Machine Engineering, 2015, Vol. 15, No. 3, p. 19-32. ISSN 1895-7595.

3. HOREJŠ, O., MAREŠ, M., HORNYCH, J. Thermal error compensation models based on transfer functions of different machine tool structures. In: EUSPEN Special Interest Group: Thermal Issues, 19-20 March 2014, Zurich, Switzerland.

4. MORÁVEK, M., BUREŠ, J., HOREJŠ, O., Volumetric measurement of machine tool thermal deformation using an MT-Check probe. In: 11th International Conference and Exhibition on Laser Metrology, Huddersfield, UK, 2015.

5. MORÁVEK, M., HOREJŠ, O., Volumetric Measurement of Five-axis Machine Tool Thermal Deformation Using an MT-Check Probe. In: EUSPEN Special Interest Group: Thermal Issues, 17-18 March 2016, Prague, Czech Republic.